SCIENCE CHINA
Information Sciences

• RESEARCH PAPER •

December 2022, Vol. 65 222202:1–222202:18
https://doi.org/10.1007/s11432-022-3561-2

Robust adaptive repetitive control for unknown linear systems with odd-harmonic periodic disturbances

Edi KURNIAWAN[1], Hendra G. HARNO[2], Hai WANG[3*], Jalu A. PRAKOSA[1], Bernadus H. SIRENDEN[4], Harry SEPTANTO[5], Hendra ADINANTA[6] & Akif RAHMATILLAH[7]

[1]*Research Center for Photonics, National Research and Innovation Agency, Tangerang Selatan* 15314*, Indonesia;*
[2]*Faculty of Science and Technology, Sanata Dharma University, Yogyakarta* 55281*, Indonesia;*
[3]*Discipline of Engineering and Energy, Murdoch University, Perth* 6150*, Australia;*
[4]*Research Center for Electronics, National Research and Innovation Agency, Bogor* 15314*, Indonesia;*
[5]*Research Center for Smart Mechatronics, National Research and Innovation Agency, Bogor* 40135*, Indonesia;*
[6]*Research Center for Hydrodynamics Technology, National Research and Innovation Agency, Surabaya* 60112*, Indonesia;*
[7]*Faculty of Science and Technology, Airlangga University, Surabaya* 60115*, Indonesia*

Received 16 February 2022/Revised 12 June 2022/Accepted 4 July 2022/Published online 4 November 2022

Abstract This article presents a novel tracking control strategy for unknown linear systems perturbed by odd-harmonic periodic disturbances that combine adaptive and repetitive control methods. The proposed control strategy results in a robust adaptive odd-harmonic repetitive controller (RA-OHRC). Direct adaptive control with a robust adaptation law is utilized to accurately track the desired trajectory, ensuring the boundedness and convergence of the tracking error. An internal-model-based repetitive controller is added to compensate for periodic disturbances with odd-harmonic components. The boundedness and the convergence of the tracking error are verified through the Lyapunov-based stability analysis. The effectiveness of the proposed RA-OHRC scheme can be demonstrated using the simulation studies involving a servomotor model, which achieves accurate reference tracking, excellent disturbance rejection capability, and robustness against uncertainties.

Keywords repetitive control, direct adaptive control, odd-harmonic frequencies, periodic disturbances, unknown linear systems

Citation Kurniawan E, Harno H G, Wang H, et al. Robust adaptive repetitive control for unknown linear systems with odd-harmonic periodic disturbances. Sci China Inf Sci, 2022, 65(12): 222202, https://doi.org/10.1007/s11432-022-3561-2

1 Introduction

Periodic compensation against repetitive disturbances is a control task commonly found in many applications such as rotation machines [1,2], power inverters [3,4], marine vessels [5], wind-turbines [6], hydraulic systems [7], and space stations [8]. A repetitive control (RC) method is a popular technique for periodic reference tracking and/or disturbance rejection. In designing the RC system, one generally requires two basic information: (1) a plant model and (2) a reference/disturbance model. A known disturbance model is embedded as part of the resulting controller to generate RC signals to compensate for the disturbance signals. Using the reference/disturbance model within a feedback control loop is referred to as an internal model principle [9]. Furthermore, the RC requires a plant model used to synthesize a compensator, determines the stability of the resulting RC closed-loop system, and dictates how fast the disturbance signals can be canceled.

A traditional RC is generally structured by a one-period delay z^{-N} with positive feedback forming an internal model of $z^{-N}/[1 - z^{-N}]$. Here, N represents an integer defined as the number of samples

* Corresponding author (email: hai.wang@murdoch.edu.au)

per disturbance period T_w. This internal model gives a null tracking error for a disturbance signal with frequencies of n/T_w, where $n = 1, 2, \ldots, N/2$ [10]. In other words, this model can compensate for a fundamental frequency, even- and odd-harmonic components up to the Nyquist frequency of the disturbance signal. This is due to the internal model $z^{-N}/[1 - z^{-N}]$ providing infinite gains at those frequencies.

In many practical applications, reference and disturbance signals generally exhibit odd-harmonic frequencies. Those applications can be found in power systems [11, 12], magnetically-suspended rotor systems [13, 14], field-modulated magnetometer systems [15], nano-positioning systems [16], and centrifugal compressors [17]. Considering this, we can avoid using the traditional RC if we only intend to target the odd-harmonic periodic disturbances. The traditional RC also introduces infinite gains at even harmonics, which reduces system robustness and degrades the system performance [18]. Furthermore, the traditional RC easily induces instability due to plant model uncertainties and slow transient responses due to the one-cycle delay term.

To overcome the above limitations of the traditional RC, a new approach based on the odd-harmonic repetitive control (OHRC) and the robust adaptive control (RAC) is considered. In this approach, the OHRC employs a specific internal model representing the disturbance model at only the odd-harmonic frequencies. Thus, instead of using the traditional RC, it is reasonable to use the OHRC to appropriately cancel the odd-harmonic periodic disturbances. Moreover, the OHRC uses a half-cycle delay compared to the traditional RC requiring a one-cycle delay to generate the control signal. Meanwhile, the RAC is added to complement the OHRC to provide accurate reference tracking and strong robustness against unknown plant dynamics and uncertainties. This is reasonable because the stability of the RC-type controlled system is easily affected by the unmodeled dynamics and plant uncertainties.

Some related results using the adaptive/robust control and the learning-based control can be found in [19–27]. In [19], an adaptive neural tracking controller with nonstrict-feedback form and prespecified tracking accuracy was designed for a class of uncertain stochastic nonlinear systems. Wu et al. [20] addressed the adaptive fuzzy tracking problem for a class of nonlinear pure-feedback systems with a quantized input signal. A robust RC design based on output-feedback control for a class of linear time-varying systems with structured uncertainties was developed in [21]. Kurniawan et al. [22] presented a sliding mode-based RC for tracking control of the linear systems subject to the exogenous periodic disturbances and plant parametric uncertainties. In [23], an adaptive repetitive scheme was developed using a robust integral of the sign of error feedback control to handle the periodic and unmodeled disturbances in an electro-hydraulic load simulator. Chen et al. [24] proposed an adaptive repetitive learning control method for permanent magnet synchronous servomotor systems with bounded nonparametric uncertainties. Ref. [25] designed a control strategy incorporating the repetitive learning method and the adaptive technique for a mobile-wheeled inverted pendulum subject to periodic disturbances and parametric uncertainties. An adaptive repetitive contouring controller to compensate both periodic and non-periodic disturbances perturbing an industrial biaxial precision gantry was introduced in [26]. Further, in [27], an adaptive RC scheme was discussed to eliminate distortions caused by the unknown periodic load disturbances in the power inverter. Refs. [19, 20] discussed the tracking control problem of uncertain nonlinear systems without considering the periodic exogenous disturbances. Refs. [21–27] were concerned with tracking and/or rejecting repetitive signals in the presence of nominal system models, although the systems are also subject to different uncertainties.

Here, we focused on the problem of reference tracking and disturbance compensation of unknown linear systems perturbed by the periodic odd-harmonic disturbances. In particular, we developed a control strategy utilizing robust adaptive odd-harmonic repetitive control (RA-OHRC) scheme. The RAC refers to a model-reference adaptive control technique, applying a robust adaptation law to perform tracking control of the linear systems with unknown plant models. The adaptation parameters are updated online to produce a bounded control signal and ensure the convergence of the tracking error. Meanwhile, the odd-harmonic repetitive control referred to as the OHRC is added to suppress the periodic disturbance at its odd-harmonic components. Notably, the design of the OHRC does not require plant dynamics anymore. This approach generally contrasts the design of feedback RC systems. Simulation results and comparison studies are provided to highlight the effectiveness of the proposed control method. In order to emphasize the novelty of this research, the main contributions are summarized as follows.

(1) A new control scheme combining the RAC and the OHRC methods is established. The OHRC is employed to significantly suppress the odd-harmonic periodic disturbances. Furthermore, compared to the traditional RC, the OHRC cancels the odd-harmonic periodic disturbances and provides a faster

transient response due to the use of a half-cycle delay in the design. Meanwhile, the RAC is added to provide accurate reference tracking and strong robustness against the unknown linear system. Moreover, the RAC can handle the parameter uncertainties.

(2) Since the plant model is assumed to be unknown, the RC method we proposed here is referred to as a model-free RC method. In contrast, the traditional RC method requires the plant model information to synthesize the compensator and ensure the stability of the resulting RC-controlled system.

(3) To assess the stability of the resulting closed-loop system, we introduced the estimation error dynamics consisting of three different errors: the repetitive error, the parameter-α error, and the parameter-β error. A Lyapunov function used in the stability analysis is then constructed based on those three errors. Then, we showed that the boundedness of the system signals and the convergence of the tracking error are guaranteed.

The remainder of this paper is organized as follows. In Section 2, the problem statement and some assumptions are presented. Section 3 discusses a new control method combining the robust adaptive and the odd-harmonic repetitive control schemes. A stability analysis involving the Lyapunov function is established in Section 4. A numerical example is given in Section 5. Finally, Section 6 includes concluding remarks.

2 Problem statement

In this paper, we consider a class of linear-time invariant (LTI) systems represented as follows:

$$y(k) = [P(z)]\, u(k) + w(k), \tag{1}$$

where $y(k), u(k), w(k) \in \mathbb{R}$ denote a plant output, a control input, and a periodic exogenous disturbance, respectively, and $P(z)$ is an unknown plant model. The unknown plant model $P(z)$ is considered to have the following expression:

$$P(z) = k_p \frac{B(z)}{A(z)}, \tag{2}$$

where k_p is a plant gain, and $B(z)$ and $A(z)$ are plant numerator and denominator polynomials, respectively, which are given by

$$B(z) = z^q + b_1 z^{q-1} + \cdots + b_{q-1} z + b_q, \tag{3}$$

$$A(z) = z^p + a_1 z^{p-1} + \cdots + a_{p-1} z + a_p. \tag{4}$$

Here, the plant parameters $k_p, a_1, \ldots, a_p, b_1, \ldots, b_q$ are considered to be unknown, while the numerator degree q and the denominator degree p are known. Next, we also consider the reference LTI system given as

$$y_r(k) = z^{-n} r(k), \tag{5}$$

where $r(k)$ is a reference input and $y_r(k)$ is a reference output. Here, z^{-n} is an input delay with the length of n. Note that z is referred to as the $\mathcal{Z}$-transform variable and also as the forward-shifting operator, e.g., $zr(k) = r(k+1)$. In addition, z^{-1} represents a backward-shifting operator, e.g., $z^{-1}r(k) = r(k-1)$. The input delay z^{-n} is particularly defined as a reference model $M(z)$. That is,

$$M(z) = z^{-n}. \tag{6}$$

The reference model $M(z)$ other than z^{-n}, as long as its transfer function has a relative degree n, can be used as the reference. For the sake of simplicity, we prefer a reference model (6) since the reference output $y_r(k)$ is simply a delayed version of the reference input $r(k)$ by the delay length of n samples. Moreover, we also define a tracking error $e(k)$ as

$$e(k) := y_r(k) - y(k) = r(k-n) - y(k). \tag{7}$$

For the unknown linear system (1), we thus intend to construct the control input $u(k)$ such that: (1) the periodic disturbance $w(k)$ is rejected; (2) the plant output $y(k)$ precisely follows the reference output $y_r(k)$; (3) the tracking error $e(k)$ asymptotically converges to zero steady-state; and (4) the resulting closed-loop system is stable and robust against plant uncertainties. To ensure that these objectives are achievable, we necessarily define several assumptions as follows.

Assumption 1. The exogenous disturbance $w(k)$ is periodic with a known fundamental frequency f_w. This gives a basis period of $T_w = \frac{1}{f_w}$. In addition, it is possible that the disturbance $w(k)$ contains odd-harmonic frequencies.

Assumption 2. The unknown plant $P(z)$ is stable and minimum phase. This implies that $B(z)$ and $A(z)$ in (2) are stable polynomials. In addition, the polynomials $B(z)$ and $A(z)$ are co-prime.

Assumption 3. The plant parameters $k_p, a_1, \ldots, a_p, b_1, \ldots, b_q$ are unknown. However, the sign of k_p, the degrees p and q of the polynomials $A(z)$ and $B(z)$ are assumed to be known, respectively. It also assumed that $|k_p| < k_p^0$ for some positive constant k_p^0.

Assumption 4. The reference model $M(z)$ is chosen such that $n < p$ and $n = p - q$.

Remark 1. Note that Assumptions 1 and 4 are needed to design the OHRC, and Assumptions 2–4 are required to synthesize the RAC. Here, Assumption 1 is used to design the internal model part of RC, while Assumption 4 is utilized to construct the compensator part. Assumptions 2–4 give detailed specifications of the plant and reference model, which determine the dimension of the adaptive parameters constructing the RAC law. In addition, Assumptions 2–4 have become standard assumptions in the design of discrete-time model reference adaptive control [28, 29].

3 Proposed method

In this section, we present a control strategy by combining the robust adaptive control and the odd-harmonics repetitive control methods in order to generate the desirable control input $u(k)$ for the linear system (1). Thus, the proposed control strategy is referred to as the RA-OHRC, which results in the control input $u(k)$ expressed as

$$u(k) = u_A(k) + u_R(k), \tag{8}$$

where $u_A(k)$ and $u_R(k)$ are the control signals generated from the adaptive and repetitive control schemes, respectively.

3.1 Robust adaptive control

We first design the adaptive control law $u_A(k)$, which is adopted from a model reference adaptive control method presented in [29]. The control law $u_A(k)$ is then given by

$$u_A(k) = \alpha_1^{\mathrm{T}}(k) \left[\frac{\mu(z)}{\lambda(z)}\right] u(k) + \alpha_2^{\mathrm{T}}(k) \left[\frac{\mu(z)}{\lambda(z)}\right] y(k) + \alpha_3(k) y(k) + \alpha_4(k) r(k), \tag{9}$$

where $\{\alpha_1(k), \alpha_2(k)\} \in \mathbb{R}^{p-1}$ and $\{\alpha_3(k), \alpha_4(k)\} \in \mathbb{R}$ are adaptive parameters, $\lambda(z)$ is a stable polynomial with a degree of $p-1$, and $\mu(z)$ is described as

$$\mu(z) = \begin{cases} 0, & \text{if} \quad p < 2, \\ \left[z^{p-2}, \ldots, z, 1\right]^{\mathrm{T}}, & \text{if} \quad p \geqslant 2. \end{cases} \tag{10}$$

Remark 2. Eq. (9) shows that the RAC law is divided into four parts with different adaptive parameters (i.e., $\alpha_1(k)$–$\alpha_4(k)$). In addition, four different input signals (i.e., the reference input $r(k)$, the plant output $y(k)$, the filtered output $\frac{\mu(z)}{\lambda(z)} y(k)$ and the filtered control signal $\frac{\mu(z)}{\lambda(z)} u(k)$) are paired to construct the control law $u_A(k)$. This control law becomes the common form in the design of discrete-time model reference adaptive control as shown in [28, 29].

Note that $\alpha_1^{\mathrm{T}}(k), \alpha_2^{\mathrm{T}}(k), \alpha_3(k), \alpha_4(k)$ are respectively estimates of the true parameters $\alpha_1^{*\mathrm{T}}, \alpha_2^{*\mathrm{T}}, \alpha_3^*, \alpha_4^*$ at time k. To simplify (9), we then define $\boldsymbol{\alpha}(k)$ and $\boldsymbol{\omega}(k)$ as follows:

$$\boldsymbol{\alpha}(k) = \left[\alpha_1^{\mathrm{T}}(k) \ \alpha_2^{\mathrm{T}}(k) \ \alpha_3(k) \ \alpha_4(k)\right]^{\mathrm{T}}, \quad \boldsymbol{\alpha}(k) \in \mathbb{R}^{2p}, \tag{11}$$

$$\boldsymbol{\omega}(k) = \left[\tfrac{\mu(z)}{\lambda(z)} u(k) \ \tfrac{\mu(z)}{\lambda(z)} y(k) \ y(k) \ r(k)\right]^{\mathrm{T}}, \quad \boldsymbol{\omega}(k) \in \mathbb{R}^{2p}, \tag{12}$$

such that

$$u_A(k) = \boldsymbol{\alpha}^{\mathrm{T}}(k) \boldsymbol{\omega}(k). \tag{13}$$

We also introduce an adaptive parameter $\beta(k) \in \mathbb{R}$ used to construct an estimation error $\epsilon(k) \in \mathbb{R}$ as follows:

$$\epsilon(k) = e(k) + \beta(k)\xi(k), \tag{14}$$

where $e(k)$ is the tracking error as defined in (7) and $\xi(k)$ is given by

$$\xi(k) = \left[\boldsymbol{\alpha}^{\mathrm{T}}(k)\boldsymbol{\omega}(k-n) - \boldsymbol{\alpha}^{\mathrm{T}}(k-n)\boldsymbol{\omega}(k-n)\right]. \tag{15}$$

The adaptive parameters $\boldsymbol{\alpha}(k)$ in (11) and $\beta(k)$ in (14) are updated using normalized gradient algorithm with parameter projection as follows [29]:

$$\boldsymbol{\alpha}(k+1) = \boldsymbol{\alpha}(k) + \frac{\mathrm{sgn}(k_p)\epsilon(k)\Gamma\boldsymbol{\omega}(k-n)}{n_\omega^2(k)} + \boldsymbol{f}_\alpha(k), \tag{16}$$

$$\beta(k+1) = \beta(k) + \frac{\gamma\epsilon(k)\xi(k)}{n_\omega^2(k)} + f_\beta(k). \tag{17}$$

To further describe the robust adaptation schemes (16) and (17), some details are then provided as follows:

$$\Gamma \in \mathbb{R}^{2p\times 2p}, \quad \Gamma = \Gamma^{\mathrm{T}}, \quad 0 < \Gamma < \frac{2}{k_p^0} I_{2p}, \tag{18}$$

$$n_\omega^2(k) \in \mathbb{R}, \quad n_\omega^2(k) = 1 + \boldsymbol{\omega}^{\mathrm{T}}(k-n)\Gamma\boldsymbol{\omega}(k-n), \tag{19}$$

$$\gamma \in \mathbb{R}_{>0}, \quad 0 < \gamma < 2, \tag{20}$$

$$f_{\alpha_i}(k) \in \mathbb{R}, \quad f_{\alpha_i}(k) = \begin{cases} 0, & \text{if } \alpha_i - g_{\alpha_i} \in [\alpha_i^l, \alpha_i^u], \\ \alpha_i^u - \alpha_i - g_{\alpha_i}, & \text{if } \alpha_i - g_{\alpha_i} > \alpha_i^u, \\ \alpha_i^l - \alpha_i - g_{\alpha_i}, & \text{if } \alpha_i - g_{\alpha_i} < \alpha_i^l, \end{cases} \tag{21}$$

$$f_\beta(k) \in \mathbb{R}, \quad f_\beta(k) = \begin{cases} 0, & \text{if } \beta - g_\beta \in [\beta^l, \beta^u], \\ \beta^u - \beta - g_\beta, & \text{if } \beta - g_\beta > \beta^u, \\ \beta^l - \beta - g_\beta, & \text{if } \beta - g_\beta < \beta^l, \end{cases} \tag{22}$$

$$\boldsymbol{g}_{\boldsymbol{\alpha}}(k) \in \mathbb{R}^{2p}, \quad \boldsymbol{g}_{\boldsymbol{\alpha}}(k) = \frac{\epsilon(k)\Gamma\boldsymbol{\omega}(k-n)}{n_\omega^2(k)}, \tag{23}$$

$$g_\beta(k) \in \mathbb{R}, \quad g_\beta(k) = \frac{\gamma\epsilon(k)\xi(k)}{n_\omega^2(k)}. \tag{24}$$

Note that $\boldsymbol{f}_\alpha(k)$ in (16) and $f_\beta(k)$ in (17) are projection functions of parameters $\boldsymbol{\alpha}(k)$ and $\beta(k)$ as detailed in (21) and (22), respectively. Here, $n_\omega(k)$ is a normalizing signal, and Γ and γ are some chosen adaptation gains. In addition, α_i and g_{α_i} are the i-th components of vectors $\boldsymbol{\alpha}(k)$ and $\boldsymbol{g}_{\boldsymbol{\alpha}}(k)$, respectively. The variables α_i^u and α_i^l represent the upper and lower bounds of $\alpha_i(k)$. Similarly, β^u and β^l denote the upper and lower bounds of $\beta(k)$. The true parameters $\boldsymbol{\alpha}^*$ and β^* are considered inside the bounds. That is,

$$\boldsymbol{\alpha}^* \in [\boldsymbol{\alpha}^l, \boldsymbol{\alpha}^u], \quad \beta^* \in [\beta^l, \beta^u]. \tag{25}$$

3.2 Odd-harmonic repetitive control

We now present the odd-harmonic repetitive control law $u_R(k)$ expressed as follows:

$$u_R(k) = \underbrace{\left[\frac{-z^{-N/2}}{1+z^{-N/2}}\right]}_{\text{Internal model}} C(z) \left[\frac{\epsilon(k)}{n_\omega^2(k)}\right], \tag{26}$$

where $[\frac{-z^{-N/2}}{1+z^{-N/2}}]$ corresponds to an RC internal model as in [18], $C(z)$ is an RC compensator, $\epsilon(k)/n_\omega^2(k)$ is defined as a normalized estimation error and becomes an input signal to the RC, and $N \in \mathbb{Z}$ is the

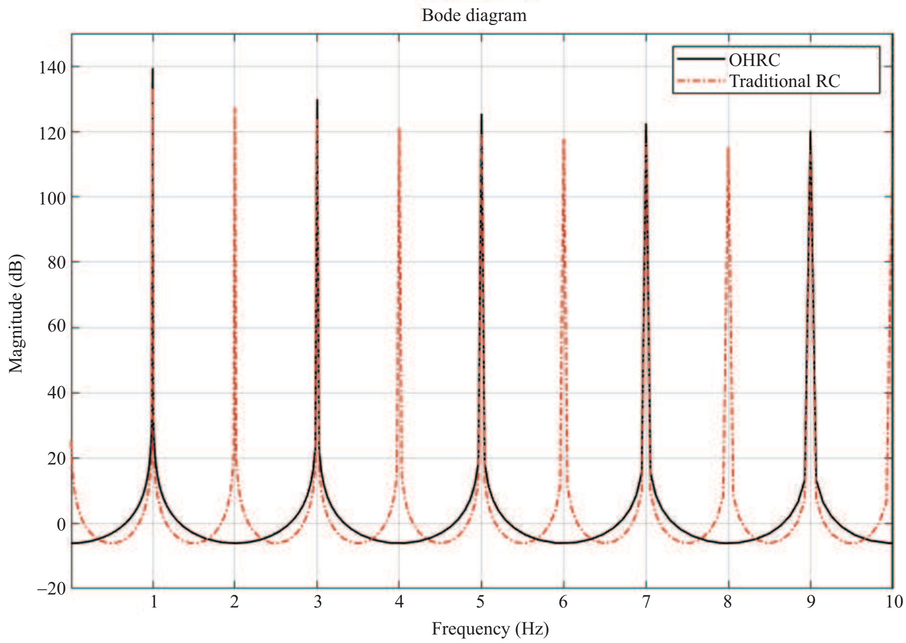

Figure 1 (Color online) Magnitude responses of the internal models of OHRC and traditional RC with a fundamental frequency of 1 Hz.

number of samples per disturbance period. It can be seen that the repetitive control law (26) uses the normalized estimation error $\epsilon(k)/n_\omega^2(k)$ as the input. This is to follow the adaptation algorithms (16) and (17) that utilize the similar error. In this way, the stability analysis of the closed-loop system with the proposed controller can be properly established. Here, N is an integer number given by

$$N = \frac{T_w}{T}, \tag{27}$$

where T_w is the fundamental disturbance period and T is a sampling period.

Remark 3. Supporting Assumption 1, the priori information about the disturbance period T_w is required to compute the integer N, which can be seen in (27). This priori information is a standard assumption used in the design of repetitive controller [11–17]. In case that the period information is unknown, then the period identification can be performed beforehand using certain algorithms such as in [30, 31].

The internal model in (26) represents the disturbance models at the odd-harmonic frequencies only such that $f \in [f_w, 3f_w, 5f_w, \ldots]$. This is illustrated in Figure 1 showing the magnitude responses of the OHRC and the traditional RC with a fundamental frequency of 1 Hz. Hence, it is obvious that only the disturbances at odd harmonics are to be rejected. In the RC-controlled system, a compensator is commonly required to stabilize the resulting closed-loop system and also determines the rate of disturbance rejection. The compensator $C(z)$ is then formulated as

$$C(z) = k_r M^{-1}(z), \tag{28}$$

where k_r is an RC gain and $M^{-1}(z)$ is an inverse of the reference model (6). We notice in (28) that when designing the compensator $C(z)$, the plant model $P(z)$ written in (2), which is unknown, is not required. This is in contrast to the general feedback RC which requires the plant model to be known to design the corresponding compensator. Thus, as shown in (28), the compensator $C(z)$ is instead obtained by using the reference model $M(z)$, which can freely be chosen as long as Assumption 4 is satisfied. We thus consider that the RC design in (26) is a model-free repetitive controller.

Now, based on (9), (14), (15), (26), a closed-loop system can be formed and the corresponding controller is referred to as the RA-OHRC. Such a controller consists of three main blocks, namely the RAC, the OHRC, and the estimation error as depicted in Figure 2.

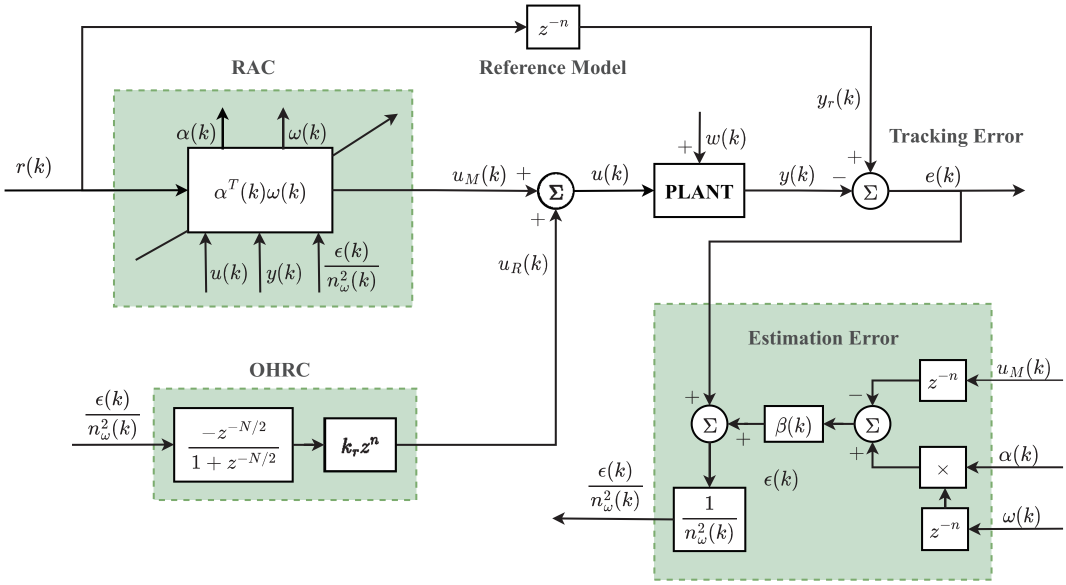

Figure 2 (Color online) A closed-loop system with the proposed RA-OHRC.

4 Stability analysis

Having the closed-loop system as shown in Figure 2, we now present a stability analysis, which includes plant-reference dynamics matching and estimation error dynamics, using the Lyapunov stability approach.

4.1 Dynamics matching

First, we consider that there are solutions or true parameters $\boldsymbol{\alpha}^* = [\alpha_1^{*\mathrm{T}}, \alpha_2^{*\mathrm{T}}, \alpha_3^*, \alpha_4^*]^{\mathrm{T}}$ which satisfy a matching condition in terms of a transfer function as follows:

$$\left(\frac{\alpha_4^*[k_p\frac{B(z)}{A(z)}]}{1-\alpha_1^{*\mathrm{T}}\mu(z)\frac{1}{\lambda(z)}-\alpha_2^{*\mathrm{T}}\mu(z)\frac{k_pB(z)}{\lambda(z)A(z)}-\alpha_3^*[k_p\frac{B(z)}{A(z)}]}\right)=z^{-n}. \tag{29}$$

The true parameter α_4^* is chosen as

$$\alpha_4^*=\frac{1}{k_p}, \tag{30}$$

such that the matching condition (29) can be expressed as

$$\left[\alpha_1^{*\mathrm{T}}\mu(z)-\lambda(z)\right]A(z)+\left[k_p\alpha_2^{*\mathrm{T}}\mu(z)+k_p\alpha_3^*\lambda(z)+z^n\lambda(z)\right]B(z)=0. \tag{31}$$

Since $B(z)$ and $A(z)$ are co-prime according to Assumption 2, there is a polynomial $S(z)$ satisfying

$$\left[k_p\alpha_2^{*\mathrm{T}}\mu(z)+k_p\alpha_3^*\lambda(z)+z^n\lambda(z)\right]=-S(z)A(z), \tag{32}$$

$$\left[\alpha_1^{*\mathrm{T}}\mu(z)-\lambda(z)\right]=S(z)B(z). \tag{33}$$

Multiplying (32) with $y(k)$, we then obtain

$$S(z)\left[A(z)y(k)\right]+k_p\alpha_2^{*\mathrm{T}}\mu(z)y(k)+k_p\alpha_3^*\lambda(z)y(k)=-z^n\lambda(z)y(k). \tag{34}$$

Substituting (2) into (1), we can straightforwardly rewrite the LTI system (1) as

$$A(z)y(k)=k_pB(z)u(k)+A(z)w(k). \tag{35}$$

Thus, using (35), we can recast (34) as

$$k_pS(z)B(z)u(k)+S(z)A(z)w(k)+k_p\alpha_2^{*\mathrm{T}}\mu(z)y(k)+k_p\alpha_3^*\lambda(z)y(k)=-z^n\lambda(z)y(k), \tag{36}$$

which can be rearranged after substituting (33) into (36) to yield

$$k_p\left[\alpha_1^{*\mathrm{T}}\mu(z)u(k)+\alpha_2^{*\mathrm{T}}\mu(z)y(k)+\alpha_3^*\lambda(z)y(k)\right]+S(z)A(z)w(k)=k_p\lambda(z)u(k)-z^n\lambda(z)y(k). \tag{37}$$

Dividing (37) by $k_p\lambda(z)$, we then obtain

$$\alpha_1^{*\mathrm{T}}\frac{\mu(z)}{\lambda(z)}u(k)+\alpha_2^{*\mathrm{T}}\frac{\mu(z)}{\lambda(z)}y(k)+\alpha_3^*y(k)+\frac{S(z)A(z)}{k_p\lambda(z)}w(k)=u(k)-\frac{z^n}{k_p}y(k), \tag{38}$$

which is referred to as a matching equation used to derive the estimation error dynamics.

4.2 Estimation error dynamics

To obtain the estimation error dynamics of the closed-loop system shown in Figure 2, we first need to derive the tracking error dynamics. This is begun with applying the control law (8) to matching (38) to yield

$$\alpha_1^{*\mathrm{T}}\frac{\mu(z)}{\lambda(z)}u(k)+\alpha_2^{*\mathrm{T}}\frac{\mu(z)}{\lambda(z)}y(k)+\alpha_3^*y(k)=u_A(k)+u_R(k)-\frac{S(z)A(z)}{k_p\lambda(z)}w(k)\frac{z^n}{k_p}y(k). \tag{39}$$

Using (9) and (12), and adding both sides of (39) with $\alpha_4^*\omega_4(k)$, we have

$$\begin{aligned}\alpha_1^{*\mathrm{T}}\omega_1(k)+\alpha_2^{*\mathrm{T}}\omega_2(k)+\alpha_3^*\omega_3(k)+\alpha_4^*\omega_4(k)&=\alpha_1^{\mathrm{T}}(k)\omega_1(k)+\alpha_2^{\mathrm{T}}(k)\omega_2(k)+\alpha_3(k)\omega_3(k)+\alpha_4(k)\omega_4(k)\\&\quad+\alpha_4^*\omega_4(k)+u_R(k)-\frac{S(z)A(z)}{k_p\lambda(z)}w(k)-\frac{z^n}{k_p}y(k),\end{aligned} \tag{40}$$

which can be simplified to yield

$$\alpha_4^*\omega_4(k)-\frac{z^n}{k_p}y(k)=-\left[\boldsymbol{\alpha}(k)-\boldsymbol{\alpha}^*\right]\boldsymbol{\omega}(k)+u_R(k)-\frac{S(z)A(z)}{k_p\lambda(z)}w(k). \tag{41}$$

By defining the adaptive parameter error as

$$\tilde{\boldsymbol{\alpha}}(k)=\boldsymbol{\alpha}(k)-\boldsymbol{\alpha}^*, \tag{42}$$

then Eq. (41) can be rewritten as

$$\alpha_4^*\omega_4(k)-\frac{z^n}{k_p}y(k)=-\tilde{\boldsymbol{\alpha}}(k)\boldsymbol{\omega}(k)+u_R(k)-\frac{S(z)A(z)}{k_p\lambda(z)}w(k). \tag{43}$$

Using (5), (26), and (30), and multiplying (43) with k_pz^{-n}, we obtain

$$y_r(k)-y(k)=-k_pz^{-n}\tilde{\boldsymbol{\alpha}}(k)\boldsymbol{\omega}(k)+k_pk_r\left[\frac{-z^{N/2}}{1+z^{-N/2}}\right]\frac{\epsilon(k)}{n_\omega^2(k)}-z^{-n}\frac{S(z)A(z)}{\lambda(z)}w(k). \tag{44}$$

Let $\phi(z)$ and $w_\phi(k)$ be

$$\phi(z)=z^{-n}\frac{S(z)A(z)}{\lambda(z)}, \tag{45}$$

$$w_\phi(k)=\phi(z)w(k). \tag{46}$$

Thus, by using (7), (45) and (46), Eq. (44) can be rewritten as

$$e(k)=-\,k_pz^{-n}\tilde{\boldsymbol{\alpha}}(k)\boldsymbol{\omega}(k)+k_pk_r\left[\frac{-z^{N/2}}{1+z^{-N/2}}\right]\frac{\epsilon(k)}{n_\omega^2(k)}-w_\phi(k). \tag{47}$$

Let $v(k)$ be

$$v(k)=k_{rp}\left[\frac{-z^{N/2}}{1+z^{-N/2}}\right]\frac{\epsilon(k)}{n_\omega^2(k)}, \tag{48}$$

where k_{rp} is given by

$$k_{rp} = k_r k_p. \tag{49}$$

Then Eq. (47) can be expressed as

$$e(k) = -k_p \tilde{\boldsymbol{\alpha}}(k)\boldsymbol{\omega}(k-n) + v(k) - w_\phi(k). \tag{50}$$

Eq. (50) is interpreted as the tracking error dynamics of the LTI system (1) regulated by the control law (8). Finally, the estimation error dynamics is obtained by substituting (50) into (14) such that

$$\epsilon(k) = w_\phi(k) - v(k) - \beta^* \tilde{\boldsymbol{\alpha}}(k)\boldsymbol{\omega}(k-n) - \tilde{\beta}(k)\xi(k), \tag{51}$$

where β^* and $\tilde{\beta}(k)$ are respectively given by

$$\beta^* = k_p, \tag{52}$$

$$\tilde{\beta}(k) = \beta(k) - \beta^*. \tag{53}$$

Remark 4. The term $w_\phi(k)$ in (51) is a bounded and periodic error signal to be cancelled. This property is determined based on (32), (45), and (46). Using (32), Eq. (45) can then be rewritten as

$$\phi(z) = k_p z^{-n} \alpha_2^{*\mathrm{T}} \frac{\mu(z)}{\lambda(z)} + k_p z^{-n} \alpha_3^* + 1. \tag{54}$$

Given that $\lambda(z)$ is chosen as a stable polynomial, and $\alpha_2^{*\mathrm{T}}$ and α_3^* are bounded true parameters, then $\phi(z)$ is a stable transfer function. Since $w(k)$ is periodic and $\phi(z)$ is stable, then $w_\phi(k)$ as formulated in (46) is bounded and its periodicity is preserved. However, the amplitude and phase of $w_\phi(k)$ may differ from $w(k)$.

Remark 5. The term $v(k)$ in (51) can be considered a repetitive control signal generated from (26) to compensate the periodic signal $w_\phi(k)$.

Remark 6. The estimation error (51) comprises three different errors, namely the repetitive error $\epsilon_r(k)$, the parameter-α error $\epsilon_\alpha(k)$, and the parameter-β error $\epsilon_\beta(k)$, which are respectively given by

$$\epsilon_r(k) = w_\phi(k) - v(k), \tag{55}$$

$$\epsilon_\alpha(k) = -\beta^* \tilde{\boldsymbol{\alpha}}(k)\boldsymbol{\omega}(k-n), \tag{56}$$

$$\epsilon_\beta(k) = -\tilde{\beta}(k)\xi(k). \tag{57}$$

Hence, Eq. (51) can be recast as

$$\epsilon(k) = \epsilon_r(k) + \epsilon_\alpha(k) + \epsilon_\beta(k). \tag{58}$$

Next, we prove the stability of the closed-loop system using a Lyapunov function derived from the estimation error (58).

4.3 Convergence analysis

It follows from the discussion above that a convergence condition of the LTI system (1) with the control law (8) is provided as follows.

Theorem 1. Consider the closed-loop system consisting of the unknown LTI system (1) with the periodic disturbance $w(k)$ under Assumptions 1–4, the adaptive controller designed using (9) with the adaptation law (16) and (17), and the repetitive controller given by (26). Then, there exists a positive constant σ such that the resulting closed-loop system is stable in the sense that the estimation error $\epsilon(k)$ is bounded and decays to the zero steady state. This condition also implies that the tracking error $e(k)$ is a bounded decaying signal.

Proof. Let us choose this candidate of Lyapunov function:

$$V(\epsilon_r, \epsilon_\alpha, \epsilon_\beta) = V_1(\epsilon_r(k)) + V_2(\epsilon_\alpha(k)) + V_3(\epsilon_\beta(k)), \tag{59}$$

where

$$V_1(\epsilon_r(k)) = k_{rp}^{-1} \sum_{h=k}^{k+N/2-1} \epsilon_r^2(h), \tag{60}$$

$$V_2(\epsilon_\alpha(k)) = |\beta^*| \tilde{\boldsymbol{\alpha}}^{\mathrm{T}}(k) \Gamma^{-1} \tilde{\boldsymbol{\alpha}}(k), \tag{61}$$

$$V_3(\epsilon_\beta(k)) = \gamma^{-1} \tilde{\beta}^2(k). \tag{62}$$

To obtain the time difference of the quadratic function $V_1(\epsilon_r(k))$, we need to apply the properties of $w_\phi(k)$ and $v(k)$ as follows:

$$w_\phi(k+N/2) = -w_\phi(k), \tag{63}$$

$$w_\phi^2(k+N/2) = w_\phi^2(k), \tag{64}$$

$$v(k) + v(k+N/2) = -k_{rp} \frac{\epsilon(k)}{n_\omega^2(k)}. \tag{65}$$

The property (63) holds for any discrete-time periodic signal with a fundamental period of $T_w = NT$ [18]. The properties (64) and (65) straightforwardly follow from (63) and (48), respectively. Now, we can have the time difference of the quadratic function $V_1(\epsilon_r(k))$ given by

$$\begin{aligned}
&V_1(\epsilon_r(k+1)) - V_1(\epsilon_r(k)) \\
&= k_{rp}^{-1} \left\{ \sum_{h=k+1}^{k+N/2} \epsilon_r^2(h) - \sum_{h=k}^{k+N/2-1} \epsilon_r^2(h) \right\} \\
&= k_{rp}^{-1} \left\{ \epsilon_r^2(k+N/2) - \epsilon_r^2(k) \right\} \\
&= k_{rp}^{-1} \left\{ \left[w_\phi(k+N/2) - v(k+N/2) \right]^2 - \left[w_\phi(k) - v(k) \right]^2 \right\} \\
&= k_{rp}^{-1} \left[v(k) + v(k+N/2) \right] \left[v(k) + v(k+N/2) + 2w_\phi(k) - 2v(k) \right] \\
&= k_{rp}^{-1} \left[v(k) + v(k+N/2) \right] \left\{ \left[v(k) + v(k+N/2) \right] + 2\epsilon_r(k) \right\} \\
&= -\frac{\epsilon(k)}{n_\omega^2(k)} \left[-k_{rp} \frac{\epsilon(k)}{n_\omega^2(k)} + 2\epsilon_r(k) \right] \\
&= \frac{\epsilon(k)}{n_\omega^2(k)} \left[k_{rp} \frac{\epsilon(k)}{n_\omega^2(k)} - 2\epsilon_r(k) \right].
\end{aligned} \tag{66}$$

Next, we intend to obtain the time differences of $V_2(\epsilon_\alpha(k))$ and $V_3(\epsilon_\beta(k))$, respectively. For this purpose, we first need to consider the following equations:

$$\tilde{\boldsymbol{\alpha}}(k+1) - \tilde{\boldsymbol{\alpha}}(k) = \boldsymbol{\alpha}(k+1) - \boldsymbol{\alpha}(k) = \frac{\mathrm{sgn}(k_p)\epsilon(k)\Gamma\boldsymbol{\omega}(k-n)}{n_\omega^2(k)} + \boldsymbol{f}_\alpha(k), \tag{67}$$

$$\tilde{\beta}(k+1) - \tilde{\beta}(k) = \beta(k+1) - \beta(k) = \frac{\gamma\epsilon(k)\xi(k)}{n_\omega^2(k)} + f_\beta(k). \tag{68}$$

Based on (16) and (67), we can have the time difference of $V_2(\epsilon_\alpha(k))$ given by

$$\begin{aligned}
&V_2(\epsilon_\alpha(k+1)) - V_2(\epsilon_\alpha(k)) \\
&= |\beta^*| \tilde{\boldsymbol{\alpha}}^{\mathrm{T}}(k+1) \Gamma^{-1} \tilde{\boldsymbol{\alpha}}(k+1) - |\beta^*| \tilde{\boldsymbol{\alpha}}^{\mathrm{T}}(k) \Gamma^{-1} \tilde{\boldsymbol{\alpha}}(k) \\
&= |\beta^*| \Gamma^{-1} \left[\tilde{\boldsymbol{\alpha}}^{\mathrm{T}}(k+1) - \tilde{\boldsymbol{\alpha}}^{\mathrm{T}}(k) \right] \tilde{\boldsymbol{\alpha}}(k+1) + |\beta^*| \Gamma^{-1} \left[\tilde{\boldsymbol{\alpha}}^{\mathrm{T}}(k+1) - \tilde{\boldsymbol{\alpha}}^{\mathrm{T}}(k) \right] \tilde{\boldsymbol{\alpha}}(k) \\
&= \left[|\beta^*| \frac{\boldsymbol{\omega}^{\mathrm{T}}(k-n)\Gamma\epsilon(k)}{n_\omega^2(k)} + |\beta^*| \boldsymbol{f}_\alpha^{\mathrm{T}}(k) \right] \times \left[\frac{\boldsymbol{\omega}(k-n)\epsilon(k)}{n_\omega^2(k)} + \Gamma^{-1}\boldsymbol{f}_\alpha(k) + 2\Gamma^{-1}\tilde{\boldsymbol{\alpha}}(k) \right] \\
&= |\beta^*| \frac{\boldsymbol{\omega}^{\mathrm{T}}(k-n)\Gamma\boldsymbol{\omega}(k-n)\epsilon^2(k)}{n_\omega^4(k)} + 2|\beta^*| \frac{\boldsymbol{\omega}^{\mathrm{T}}(k-n)\tilde{\boldsymbol{\alpha}}(k)\epsilon(k)}{n_\omega^2(k)} + |\beta^*| \boldsymbol{f}_\alpha^{\mathrm{T}}(k)\Gamma^{-1}\boldsymbol{f}_\alpha(k) \\
&\quad + 2|\beta^*| \boldsymbol{f}_\alpha^{\mathrm{T}}(k)\Gamma^{-1}\boldsymbol{g}_\alpha(k) + 2|\beta^*| \boldsymbol{f}_\alpha^{\mathrm{T}}(k)\Gamma^{-1}\tilde{\boldsymbol{\alpha}}(k)
\end{aligned}$$

$$\leqslant 2|\beta^*|\boldsymbol{f}_\alpha^{\mathrm{T}}(k)\Gamma^{-1}\left[\boldsymbol{f}_\alpha(k)+\boldsymbol{g}_\alpha(k)+\tilde{\boldsymbol{\alpha}}(k)\right]+|\beta^*|\frac{\boldsymbol{\omega}^{\mathrm{T}}(k-n)\Gamma\boldsymbol{\omega}(k-n)\epsilon^2(k)}{n_\omega^4(k)}$$
$$+2|\beta^*|\frac{\boldsymbol{\omega}^{\mathrm{T}}(k-n)\tilde{\boldsymbol{\alpha}}(k)\epsilon(k)}{n_\omega^2(k)}. \tag{69}$$

Similarly, we use (17) and (68) to obtain the time difference of $V_3(\epsilon_\beta(k))$. That is,

$$\begin{aligned}
&V_3(\epsilon_\beta(k+1))-V_3(\epsilon_\beta(k))\\
&=\gamma^{-1}\tilde{\beta}^2(k+1)-\gamma^{-1}\tilde{\beta}^2(k)\\
&=\gamma^{-1}\left[\tilde{\beta}(k+1)-\tilde{\beta}(k)\right](k+1)+\gamma^{-1}\left[\tilde{\beta}(k+1)-\tilde{\beta}(k)\right]\tilde{\beta}(k)\\
&=\left[\frac{\xi(k)\epsilon(k)}{n_\omega^2(k)}+\gamma^{-1}f_\beta(k)\right]\left[\gamma\frac{\xi(k)\epsilon(k)}{n_\omega^2(k)}+f_\beta(k)+2\tilde{\beta}(k)\right]\\
&=\gamma^{-1}f_\beta^2(k)+2\gamma^{-1}f_\beta(k)g_\beta(k)+2\gamma^{-1}f_\beta(k)\tilde{\beta}(k)+\gamma\frac{\xi^2(k)\epsilon^2(k)}{n_\omega^4(k)}+2\frac{\xi(k)\tilde{\beta}(k)\epsilon(k)}{n_\omega^2(k)}\\
&\leqslant 2\gamma^{-1}f_\beta(k)\left[f_\beta(k)+g_\beta(k)+\tilde{\beta}(k)\right]+\gamma\frac{\xi^2(k)\epsilon^2(k)}{n_\omega^4(k)}+2\frac{\xi(k)\tilde{\beta}(k)\epsilon(k)}{n_\omega^2(k)}.
\end{aligned} \tag{70}$$

The time increment of $V(\epsilon_r(k),\epsilon_\alpha(k),\epsilon_\beta(k))$ is obtained by summing up (66), (69), and (70) such that

$$\begin{aligned}
&V(\epsilon_r(k+1),\epsilon_\alpha(k+1),\epsilon_\beta(k+1))-V(\epsilon_r(k),\epsilon_\alpha(k),\epsilon_\beta(k))\\
&\leqslant\frac{\epsilon(k)}{n_\omega^2(k)}\left[k_{rp}\frac{\epsilon(k)}{n_\omega^2(k)}-2\epsilon_r(k)\right]+|\beta^*|\frac{\boldsymbol{\omega}^{\mathrm{T}}(k-n)\Gamma\boldsymbol{\omega}(k-n)\epsilon^2(k)}{n_\omega^4(k)}\\
&\quad+2|\beta^*|\frac{\boldsymbol{\omega}^{\mathrm{T}}(k-n)\tilde{\boldsymbol{\alpha}}(k)\epsilon(k)}{n_\omega^2(k)}+\gamma\frac{\xi^2(k)\epsilon^2(k)}{n_\omega^4(k)}+2\frac{\xi(k)\tilde{\beta}(k)\epsilon(k)}{n_\omega^2(k)}\\
&\quad+2|\beta^*|\boldsymbol{f}_\alpha^{\mathrm{T}}(k)\Gamma^{-1}\left[\boldsymbol{f}_\alpha(k)+\boldsymbol{g}_\alpha(k)+\tilde{\boldsymbol{\alpha}}(k)\right]+2\gamma^{-1}f_\beta(k)\left[f_\beta(k)+g_\beta(k)+\tilde{\beta}(k)\right].
\end{aligned} \tag{71}$$

Based on (51), (55), and (21)–(24), then

$$\beta^*\boldsymbol{\omega}^{\mathrm{T}}(k-n)\tilde{\boldsymbol{\alpha}}(k)+\xi(k)\tilde{\beta}(k)=\epsilon_r(k)-\epsilon(k), \tag{72}$$
$$\boldsymbol{f}_\alpha^{\mathrm{T}}(k)\left[\boldsymbol{f}_\alpha(k)+\boldsymbol{g}_\alpha(k)+\tilde{\boldsymbol{\alpha}}(k)\right]\leqslant 0, \tag{73}$$
$$f_\beta(k)\left[f_\beta(k)+g_\beta(k)+\tilde{\beta}(k)\right]\leqslant 0 \tag{74}$$

hold. Moreover, using (72)–(74), Eq. (71) can be further expanded into

$$\begin{aligned}
&V(\epsilon_r(k+1),\epsilon_\alpha(k+1),\epsilon_\beta(k+1))-V(\epsilon_r(k),\epsilon_\alpha(k),\epsilon_\beta(k))\\
&\leqslant\frac{\epsilon(k)}{n_\omega^2(k)}\left[k_{rp}\frac{\epsilon(k)}{n_\omega^2(k)}-2\epsilon_r(k)\right]+|\beta^*|\frac{\boldsymbol{\omega}^{\mathrm{T}}(k-n)\Gamma\boldsymbol{\omega}(k-n)\epsilon^2(k)}{n_\omega^4(k)}\\
&\quad+2|\beta^*|\frac{\boldsymbol{\omega}^{\mathrm{T}}(k-n)\tilde{\boldsymbol{\alpha}}(k)\epsilon(k)}{n_\omega^2(k)}+\gamma\frac{\xi^2(k)\epsilon^2(k)}{n_\omega^4(k)}+2\frac{\xi(k)\tilde{\beta}(k)\epsilon(k)}{n_\omega^2(k)}\\
&\leqslant\frac{\epsilon(k)}{n_\omega^2(k)}\left[k_{rp}\frac{\epsilon(k)}{n_\omega^2(k)}-2\epsilon_r(k)\right]+\frac{\epsilon(k)}{n_\omega^2(k)}\left[2\epsilon_r(k)-2\epsilon(k)\right]\\
&\quad+\frac{\epsilon^2(k)}{n_\omega^2(k)}\left[|\beta^*|\frac{\boldsymbol{\omega}^{\mathrm{T}}(k-n)\Gamma\boldsymbol{\omega}(k-n)}{n_\omega^2(k)}+\gamma\frac{\xi^2(k)}{n_\omega^2(k)}\right]\\
&\leqslant\frac{\epsilon^2(k)}{n_\omega^2(k)}\left[\frac{k_{rp}}{n_\omega^2(k)}-2\right]+\frac{\epsilon^2(k)}{n_\omega^2(k)}\left[|\beta^*|\frac{\boldsymbol{\omega}^{\mathrm{T}}(k-n)\Gamma\boldsymbol{\omega}(k-n)}{n_\omega^2(k)}+\gamma\frac{\xi^2(k)}{n_\omega^2(k)}\right]\\
&\leqslant-\frac{\epsilon^2(k)}{n_\omega^2(k)}\left[2-\frac{k_{rp}}{n_\omega^2(k)}-|\beta^*|\frac{\boldsymbol{\omega}^{\mathrm{T}}(k-n)\Gamma\boldsymbol{\omega}(k-n)}{n_\omega^2(k)}-\gamma\frac{\xi^2(k)}{n_\omega^2(k)}\right]\\
&\leqslant-\sigma\frac{\epsilon^2(k)}{n_\omega^2(k)}.
\end{aligned} \tag{75}$$

where σ is given by

$$\sigma = 2 - \frac{k_{rp}}{n_{\omega}^2(k)} - |\beta^*|\frac{\boldsymbol{\omega}^{\mathrm{T}}(k-n)\Gamma\boldsymbol{\omega}(k-n)}{n_{\omega}^2(k)} - \gamma\frac{\xi^2(k)}{n_{\omega}^2(k)}. \tag{76}$$

From (75), it can be concluded that for any $\sigma > 0$, the estimation error $\epsilon(k)$ is a bounded decaying signal (i.e, $\epsilon(k) \in L^2 \cap L^\infty$), which implies that the parameter errors $\epsilon_\alpha(k), \epsilon_\beta(k)$ and the repetitive error $\epsilon_r(k)$ are bounded and decaying. This also implies that the parameters $(\boldsymbol{\alpha}(k), \beta(k))$ converge to the true values $(\boldsymbol{\alpha}^*, \beta^*)$ and the periodic disturbance $w(k)$ is cancelled. Based on (14), it is also shown that the tracking error $e(k)$ is bounded and asymptotically converges to the zero steady state. This completes the proof.

5 A numerical example

5.1 Simulation configurations

We now present an example of designing RA-OHRC for a discrete-time LTI system involving the servomotor used in [32]. The discrete-time LTI system is modeled as

$$y(k) = \frac{0.1877z + 0.1038}{z^2 - 0.9747z + 0.2662}u(k) + w(k), \tag{77}$$

where $y(k)$ is an output angle position (rad), $u(k)$ is an input voltage (V), and $w(k)$ is an output disturbance (rad). The associated sampling time for the LTI system (77) is $T = 0.05$ s. Moreover, the plant model of the LTI system shown in (77) can then be expressed as

$$P(z) = k_p\frac{z + b_1}{z^2 + a_1z + a_2}, \tag{78}$$

where $k_p = 0.1877$, $a_1 = -0.9747$, $a_2 = 0.2662$, and $b_1 = 0.5530$. It is assumed that only the degree p of the plant is known, while the true plant parameters k_p, a_1, a_2, b_1 are unknown. From (78), we thus have $p = 2$, which leads to the selection of $\boldsymbol{\alpha}(k)$'s dimension as follows:

$$\boldsymbol{\alpha}(k) = \begin{bmatrix}\alpha_1(k) & \alpha_2(k) & \alpha_3(k) & \alpha_4(k)\end{bmatrix}^{\mathrm{T}}, \quad \boldsymbol{\alpha} \in \mathbb{R}^4. \tag{79}$$

The reference input $r(k)$ is a periodic signal with the period of 1 s. Also, the disturbance signal $w(k)$ is periodic with the fundamental frequency of 1 Hz and is modeled as

$$w(k) = 0.1\sum_{j=0}^{2}\sin\left(2\pi(2j+1)\right). \tag{80}$$

The reference and disturbance signals: $r(k)$ and $w(k)$ are illustrated in Figures 3(a) and (b), respectively. Now, we can determine the reference model $M(z)$, the parameters $\mu(z)$ and $\lambda(z)$, and the initial adaptive parameters $\boldsymbol{\alpha}(0)$ as

$$M(z) = z^{-1}, \quad \mu(z) = 1, \quad \lambda(z) = z, \quad \boldsymbol{\alpha}(0) = \begin{bmatrix}0 & 0 & 0 & 0\end{bmatrix}^{\mathrm{T}}. \tag{81}$$

In addition, the adaptation gains (Γ, γ) and the $(\boldsymbol{\alpha}, \beta)$ bounds are chosen as

$$\begin{aligned}&\Gamma = \mathrm{diag}\{1.5\ 1.5\ 1.5\ 1.5\}, \quad \gamma = 1.5,\\ &[\boldsymbol{\alpha}^l, \boldsymbol{\alpha}^u] = [(-4,4),(-4,4),(-4,4),(-4,4)], \quad [\beta^l, \beta^u] = [0,5].\end{aligned} \tag{82}$$

The adaptive controller $u_A(k)$ of the form (9) can then be constructed as

$$u_A(k) = \alpha_1(k)u(k-1) + \alpha_2(k)y(k-1) + \alpha_3(k)y(k) + \alpha_4(k)r(k). \tag{83}$$

To design the repetitive controller, we first determine the integer N yielded as

$$N = \frac{T_w}{T} = \frac{1}{0.05} = 20. \tag{84}$$

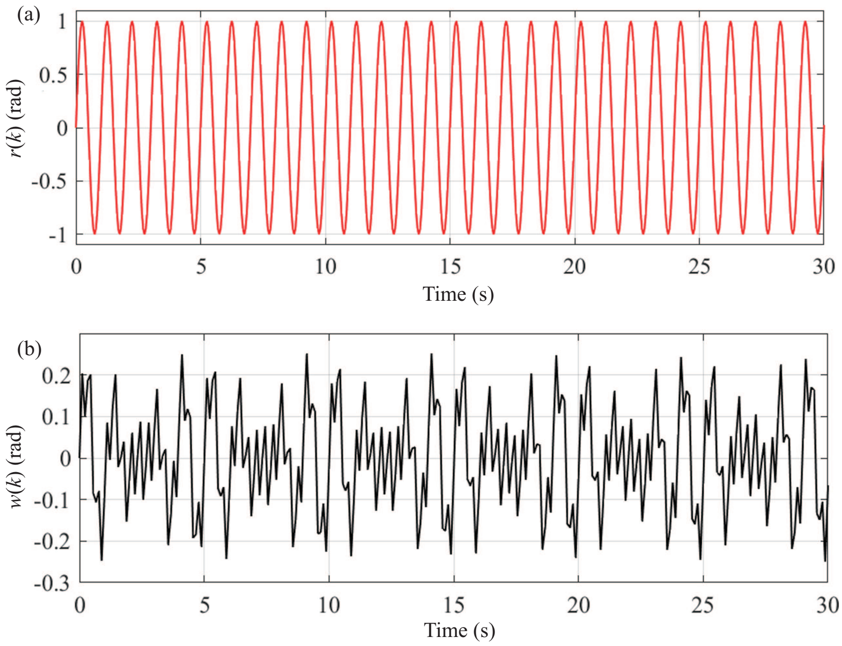

Figure 3 (Color online) (a) Reference $r(k)$; (b) disturbance $w(k)$.

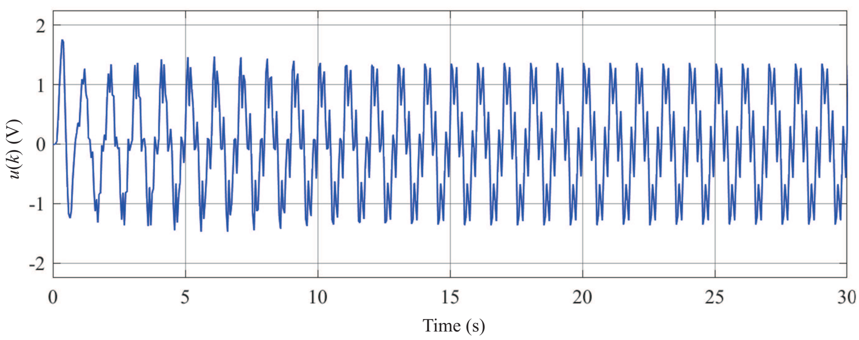

Figure 4 (Color online) Control signal $u(k)$.

Choosing the RC gain k_r as 0.75, we can have the compensator model $C(z)$ as

$$C(z) = 0.75z. \tag{85}$$

Now, the repetitive controller $u_R(k)$ of the form (26) can be designed as

$$u_R(k) = \left[-0.75\frac{z^{-9}}{1+z^{-10}}\right]\frac{\epsilon(k)}{n_w^2(k)}. \tag{86}$$

Note that $\epsilon(k)$ and $n_w^2(k)$ are calculated using (14) and (19), respectively. Finally, the proposed RA-OHRC can be synthesized from (83) and (86), which is given by

$$u(k) = u_A(k) + u_R(k). \tag{87}$$

5.2 Results and discussion

Simulation results of the LTI system (77) with the controller (87) are presented in Figures 4–8. Particularly, it is shown in Figures 4–7 that despite the presence of the unknown plant model and the external periodic disturbance, the control signal $u(k)$, the tracking error $e(k)$, the estimation error $\epsilon(k)$, and the adaptive parameters $(\boldsymbol{\alpha}(k), \beta(k))$ are all bounded. It can be seen from Figure 5 that the tracking error $e(k)$ defined as the difference between the reference output $y_r(k)$ and the plant output $y(k)$ moves

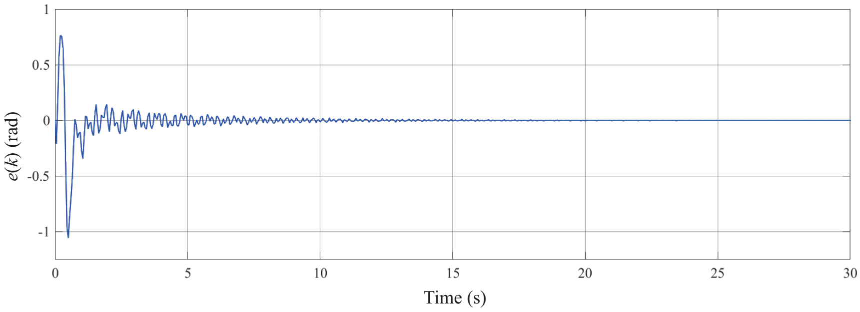

Figure 5 (Color online) Tracking error $e(k)$.

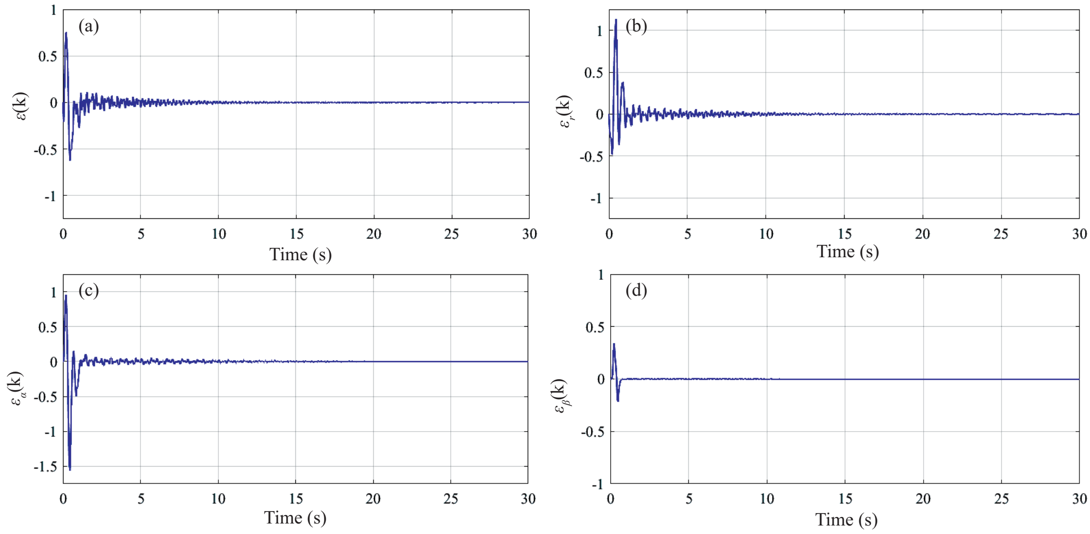

Figure 6 (Color online) Error signals. (a) Estimation error $\epsilon(k)$; (b) repetitive error $\epsilon_r(k)$; (c) parameter-α error $\epsilon_\alpha(k)$; (d) parameter-β error $\epsilon_\beta(k)$.

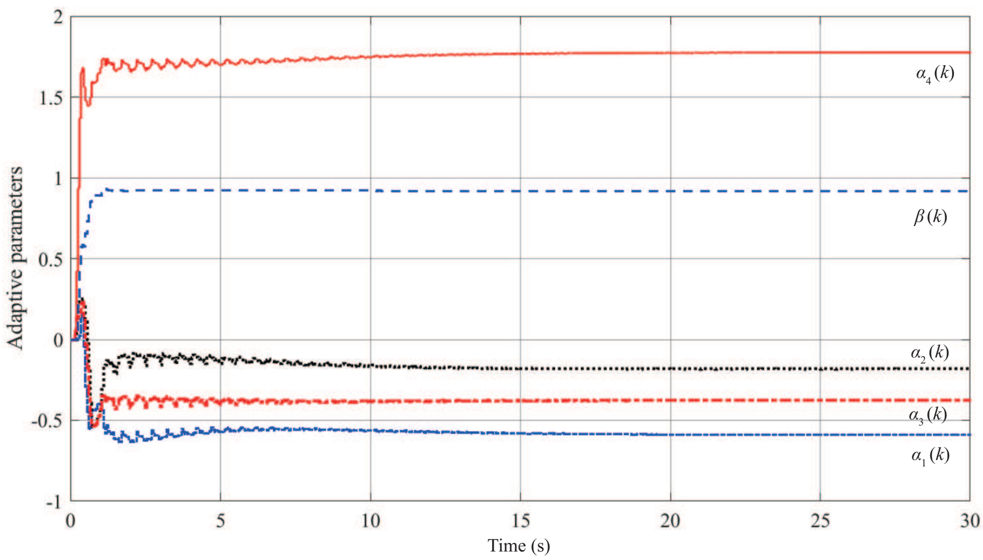

Figure 7 (Color online) Adaptive parameters $\boldsymbol{\alpha}(k)$ and $\beta(k)$.

toward zero steady-state. Similarly, the estimation error $\epsilon(k)$ in Figure 6(a) is also a decaying signal, which implies the convergence of the repetitive error $\epsilon_r(k)$ (55), the parameter-α error (56), and the parameter-β error (57). The convergences of $\epsilon_r(k)$, $\epsilon_\alpha(k)$, and $\epsilon_\beta(k)$ respectively are then confirmed in Figures 6(b)–(d). Moreover, Figure 8 illustrates the plant output $y(k)$ demonstrating the tracking capa-

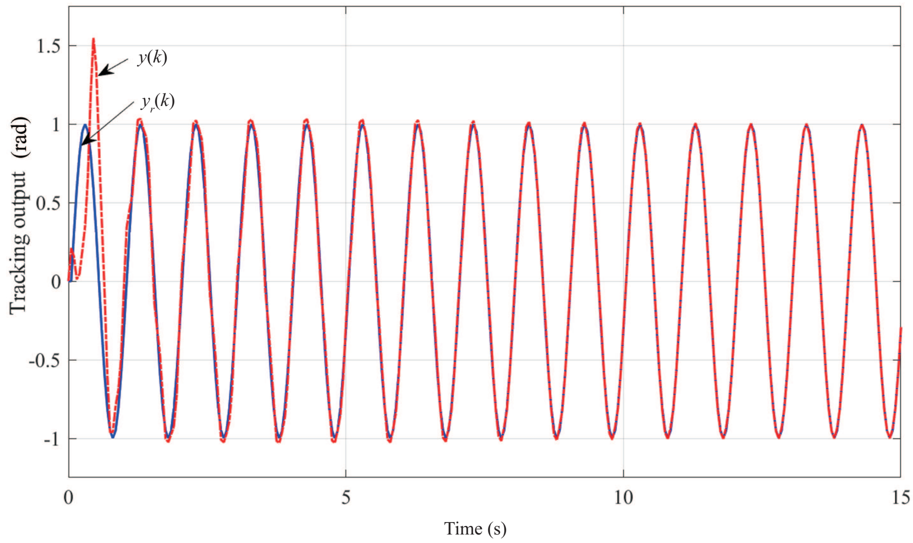

Figure 8 (Color online) Plant output $y(k)$ and reference output $y_r(k)$.

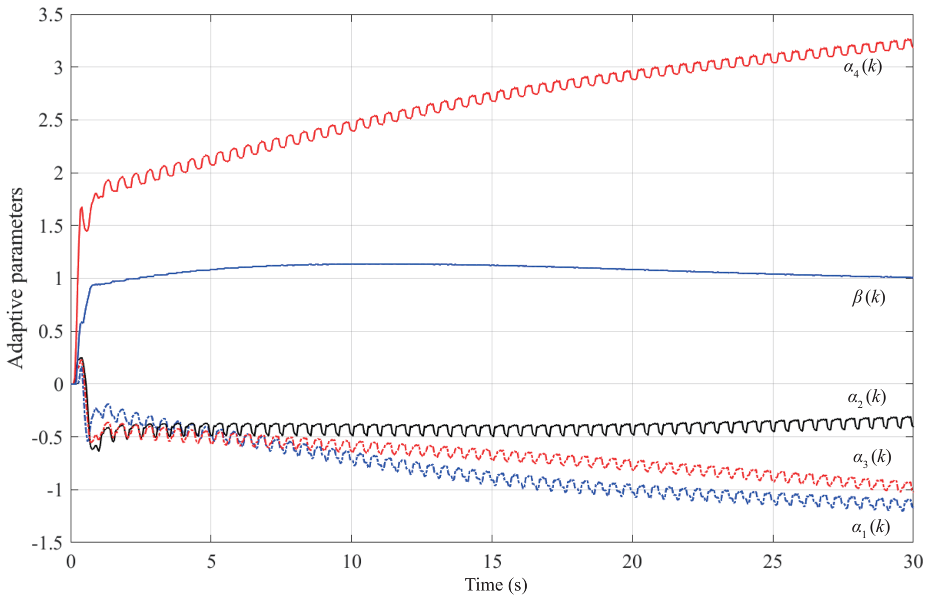

Figure 9 (Color online) Adaptive parameters $\boldsymbol{\alpha}(k)$ and $\beta(k)$ of RAC.

bility of the proposed controller. It is noticeable that the plant output $y(k)$ precisely follows the reference output $y_r(k)$ after completing the transient period. The transient period is required by the controller to adjust the adaptive parameters to cope with the unknown plant model and to generate the periodic signal for disturbance compensation. These results clearly indicate that both the reference tracking and the disturbance rejection can be achieved simultaneously.

Comparison is made to the RAC as a standalone controller. The RAC can be obtained by setting the RC gain k_r in (85) as 0. It can be seen in Figure 9 that the adaptive parameters do not converge to the true values. In addition, the time history of these parameters shows certain periodical patterns instead of the constant values. Note that the boundedness of the RAC are ensured by the adaptation laws (16) and (17). This result confirms that the adaptation parameters are greatly affected by the existence of the periodic disturbance $w(k)$.

The tracking error of the RAC is shown in Figure 10. The RAC results in a periodical bounded tracking error with no sign of convergence to the zero steady-state. This is also confirmed from the tracking output indicated in Figure 11, where the output $y(k)$ is unable to accurately follow the reference $y_r(k)$. This means that the periodic disturbance $w(k)$ remains uncancelled.

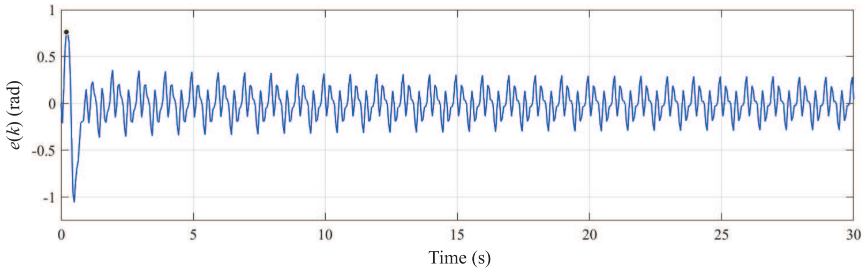

Figure 10 (Color online) Tracking error $e(k)$ of RAC.

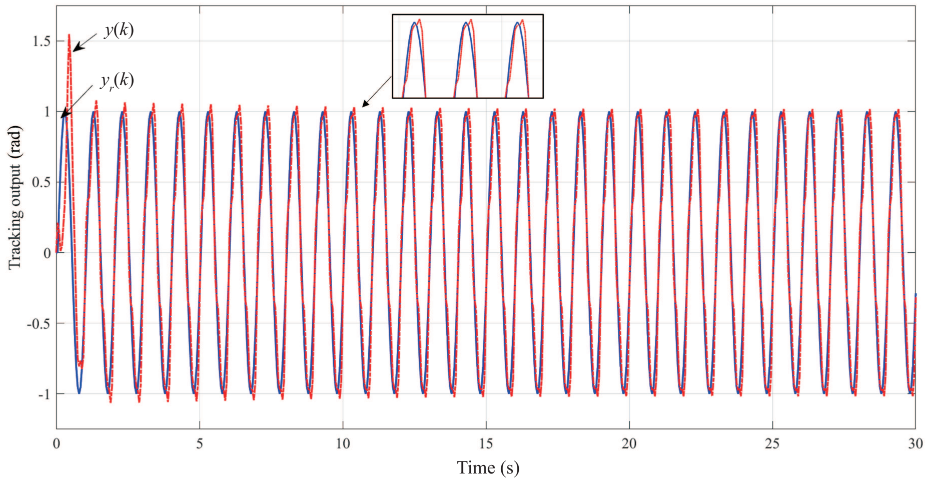

Figure 11 (Color online) Plant output $y(k)$ and reference output $y_r(k)$ of RAC.

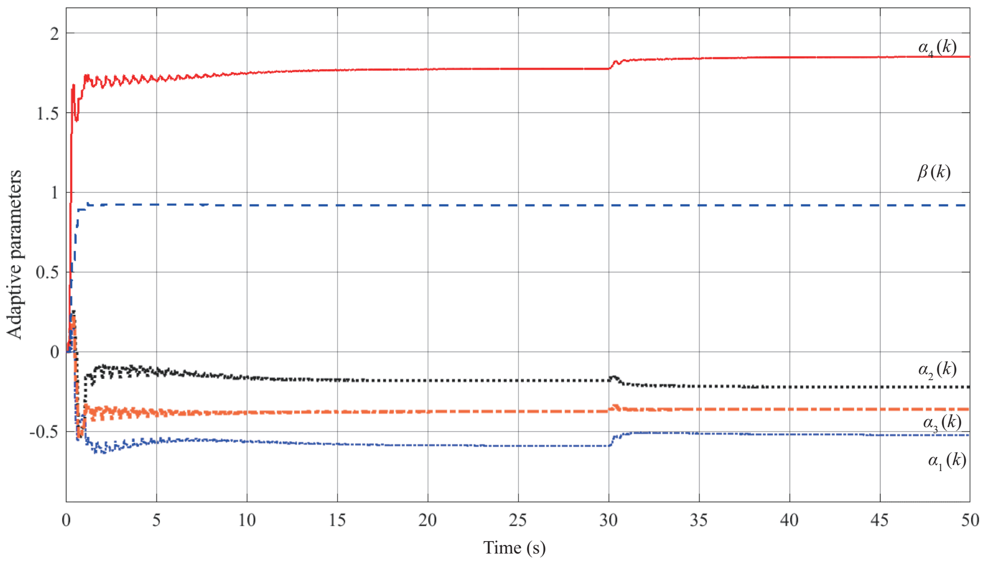

Figure 12 (Color online) Adaptive parameters $\boldsymbol{\alpha}(k)$ and $\beta(k)$ of the controlled-system with 10% plant variation.

We also examine the tracking performance of RA-OHRC when the LTI system (77) is subject to plant uncertainties. Let the 10% plant parameters variation be present at time $t > 30$ s. This gives a new plant model as

$$P_{\Delta}(z) = \frac{0.2065z + 0.1142}{z^2 - 1.0722z + 0.2928}. \tag{88}$$

This plant variation moves the system poles positions from $p_1 = 0.487 + 0.169\mathrm{j}$ and $p_2 = 0.487 - 0.169\mathrm{j}$ to the locations at $p_{1\Delta} = 0.536 + 0.073\mathrm{j}$ and $p_{2\Delta} = 0.536 - 0.073\mathrm{j}$. The new poles $p_{1\Delta}$ and $p_{2\Delta}$ are still inside

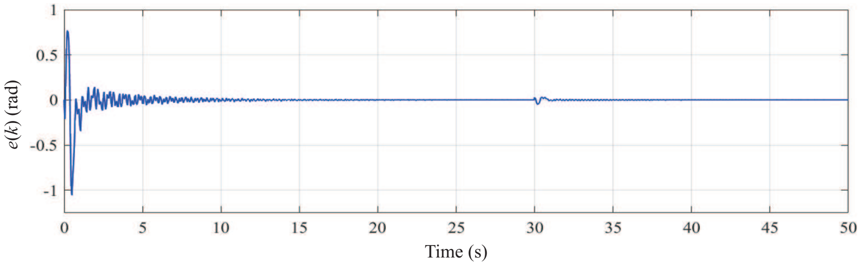

Figure 13 (Color online) Tracking error $e(k)$ of the controlled-system with 10% plant variation.

the unit circle which makes Assumption 2 remain valid. From Figure 12, we notice that the adaptive parameters at time $t = 30$ s are adjusted to the new solution. As indicated in Figure 13, this adjustment process introduces a new transition period resulting in a small transient error to the tracking error $e(k)$ before the $e(k)$ converges again to the zero steady-state. By observing behaviors shown in Figures 12 and 13, it can be concluded that the proposed algorithm is also robust against plant parameter uncertainties.

We thus infer from all the above results that a proper integration between the adaptive and the repetitive control schemes is required to handle the unknown and uncertain plant model, and to improve the tracking performance in the presence of the periodic exogenous disturbance.

6 Conclusion

We proposed a robust adaptive odd-harmonic repetitive controller for the unknown linear systems perturbed by the odd-harmonic periodic disturbances. The proposed controller design method employs direct adaptive control with the robust adaptation law to handle the unknown plant model and OHRC to eliminate the periodic exogenous disturbance. The stability analysis demonstrated that the proposed controller ensures the boundedness of the system signals and the convergence of the tracking error. Finally, the simulation results showed the effectiveness and high performance of the proposed design method.

References

1 Huo X, Wang M, Liu K Z, et al. Attenuation of position-dependent periodic disturbance for rotary machines by improved spatial repetitive control with frequency alignment. IEEE ASME Trans Mechatron, 2020, 25: 339–348
2 Cho K, Kim J, Choi S B, et al. A high-precision motion control based on a periodic adaptive disturbance observer in a PMLSM. IEEE ASME Trans Mechatron, 2015, 20: 2158–2171
3 Wang Z, Yan Y, Yang J, et al. Robust voltage regulation of a DC-AC inverter with load variations via a HDOBC approach. IEEE Trans Circ Syst II, 2019, 66: 1172–1176
4 Lai J, Yin X, Yin X, et al. Fractional order harmonic disturbance observer control for three-phase LCL-type inverter. Control Eng Pract, 2021, 107: 104697
5 Kurtoglu D, Bidikli B, Tatlicioglu E, et al. Periodic disturbance estimation based adaptive robust control of marine vehicles. Ocean Eng, 2021, 219: 108351
6 Coral-Enriquez H, Cortés-Romero J, Dorado-Rojas S A. Rejection of varying-frequency periodic load disturbances in wind-turbines through active disturbance rejection-based control. Renew Energy, 2019, 141: 217–235
7 Jia C, Longman R W. An adaptive smooth second-order sliding mode repetitive control method with application to a fast periodic stamping system. Syst Control Lett, 2021, 151: 104912
8 Iyer A, Singh S N. Non-linear momentum and attitude control of a Space Station accommodating periodic aerodynamic disturbance. Acta Astronaut, 1995, 35: 391–402
9 Francis B A, Wonham W M. The internal model principle for linear multivariable regulators. Appl Math Optim, 1975, 2: 170–194
10 Kurniawan E, Cao Z, Mahendra O, et al. A survey on robust repetitive control and applications. In: Proceedings of IEEE International Conference on Control System, Computing and Engineering (ICCSCE 2014), 2014. 524–529
11 Han B, Jo S W, Kim M, et al. Improved odd-harmonic repetitive control scheme for Ćuk-derived inverter. IEEE Trans Power Electron, 2022, 37: 1496–1508
12 Zhou K L, Low K-S, Wang D, et al. Zero-phase odd-harmonic repetitive controller for a single-phase PWM inverter. IEEE Trans Power Electron, 2006, 21: 193–201
13 Cui P, Zhang G. Modified repetitive control for odd-harmonic current suppression in magnetically suspended rotor systems. IEEE Trans Ind Electron, 2019, 66: 8008–8018
14 Cui P, Xu H, Liu Z, et al. Harmonic current suppression of magnetically suspended rotor system via odd-harmonic fractional RC. IEEE Sens J, 2019, 19: 4812–4819
15 Jeng J T, Hsu T Y, Lu C C. Odd-harmonic characteristics of the field-modulated GMR magnetometer. IEEE Trans Magn, 2011, 47: 3538–3541
16 Li L, Aphale S S, Zhu L M. Enhanced odd-harmonic repetitive control of nanopositioning stages using spectrum-selection filtering scheme for high-speed raster scanning. IEEE Trans Automat Sci Eng, 2021, 18: 1087–1096
17 Cai K, Deng Z, Peng C, et al. Suppression of harmonic vibration in magnetically suspended centrifugal compressor using zero-phase odd-harmonic repetitive controller. IEEE Trans Ind Electron, 2020, 67: 7789–7797

18 Griñó R, Costa-Castelló R. Digital repetitive plug-in controller for odd-harmonic periodic references and disturbances. Automatica, 2005, 41: 153–157
19 Wu J, Chen X, Zhao Q, et al. Adaptive neural dynamic surface control with prespecified tracking accuracy of uncertain stochastic nonstrict-feedback systems. IEEE Trans Cybern, 2022, 52: 3408–3421
20 Wu J, Wu Z G, Li J, et al. Practical adaptive fuzzy control of nonlinear pure-feedback systems with quantized nonlinearity input. IEEE Trans Syst Man Cybern Syst, 2019, 49: 638–648
21 Wu M, Zhou L, She J H, et al. Design of robust output-feedback repetitive controller for class of linear systems with uncertainties. Sci China Inf Sci, 2010, 53: 1006–1015
22 Kurniawan E, Wang H, Sirenden B H, et al. Discrete-time modified repetitive sliding mode control for uncertain linear systems. Int J Adapt Control Signal Process, 2021, 35: 2245–2258
23 Luo C, Yao J, Chen F, et al. Adaptive repetitive control of hydraulic load simulator with RISE feedback. IEEE Access, 2017, 5: 23901–23911
24 Chen Q, Yu X, Sun M, et al. Adaptive repetitive learning control of PMSM servo systems with bounded nonparametric uncertainties: theory and experiments. IEEE Trans Ind Electron, 2021, 68: 8626–8635
25 Sun W, Su S F, Xia J, et al. Adaptive tracking control of wheeled inverted pendulums with periodic disturbances. IEEE Trans Cybern, 2020, 50: 1867–1876
26 Hu C, Yao B, Chen Z, et al. Adaptive robust repetitive control of an industrial biaxial precision gantry for contouring tasks. IEEE Trans Contr Syst Technol, 2011, 19: 1559–1568
27 Tzou Y-Y, Jung S-L, Yeh H-C. Adaptive repetitive control of PWM inverters for very low THD AC-voltage regulation with unknown loads. IEEE Trans Power Electron, 1999, 14: 973–981
28 Datta A. On the transient behaviour in discrete-time model reference adaptive control: analysis and possible improvement. Automatica, 1994, 30: 527–531
29 Tao G. Adaptive Control Design and Analysis. Piscataway: Wiley-IEEE Press, 2003
30 Chang K, Shim I, Park G. Adaptive repetitive control for an eccentricity compensation of optical disk drivers. IEEE Trans Consumer Electron, 2006, 52: 445–450
31 Kim J, Lim K, Kim S. Track following control with DFT estimator for eccentric error compensation of optical disk driver. IEEE Trans Consumer Electron, 2007, 53: 467–473
32 Kurniawan E. Robust repetitive control and applications. Dissertation for Ph.D. Degree. Melbourne: Swinburne University of Technology, 2013